NONLINEAR SIMULATIONS OF SOLAR ROTATION EFFECTS IN SUPERGRANULES

DAVID H. HATHAWAY

Advanced Study Program/High Altitude Observatory, National Center for Atmospheric Research, Boulder, Colo. 80307, U.S.A.*

(Received 13 March; in revised form 2 June, 1981)

Abstract. Nonlinear calculations for the three-dimensional and time dependent convective flow in a plane parallel layer of fluid are carried out with parameter values appropriate for supergranules on the Sun. A rotation vector is used which is tilted from the vertical to represent various latitudes. For the incompressible fluid used in this model the solar rotation produces turning motions sufficient to completely twist a fluid column in about one day. It is suggested that this effect will be greatly enhanced in a compressible fluid. The tilted rotation vector produces anisotropies and systematic Reynolds stresses which drive mean flows. The resulting flows produce a rotation rate which increases inward and a meridional circulation with poleward flow along the outer surface.

1. Introduction

Supergranulation was originally identified with convection by Leighton *et al.* (1962). Although Hart (1954, 1956) was the first to report the existence of these large scale velocity patterns she in fact dismissed the possibility that it is a convective phenomenon. Observations show a cellular pattern of horizontal velocities of about 300 m s^{-1} in the photosphere. These motions diverge from the cell centers and converge at the boundaries which are cospatial with the chromospheric network. Typical cell diameters are about 30 000 km. The nature of the flows and the large cell diameters led Leighton *et al.* (1962) to suggest that the motions are convective and originate deep within the Sun. Since that time a number of observations have refined the statistics for the motions and several theoretical studies have been done on the role of magnetic fields in these cells. Very little work, however, has been done on the effects of solar rotation on the motions.

Solar rotation is often thought to be too slow to substantially affect the convective flow in supergranulation cells. The Sun's rotation period is some twenty to thirty times longer than a turnover time for the supergranules. This would suggest that any effect due to rotation should be minor. Similar arguments can be made about cumulus convection in the Earth's atmosphere and yet these storms are infamous for spawning tornadoes with intense twisting motions. An analogy such as this may seem inappropriate since moisture, precipitation, and ambient wind shears play inportant roles in the Earth's atmosphere and probably have no counterparts on the Sun. However, such a comparison does illustrate the importance of examining the possible effects of rotation before dismissing them a priori.

* The National Center for Atmospheric Research is sponsored by the National Science Foundation.

Solar Physics **77** (1982) 341–356. 0038–0938/82/0772–0341 $02.40.

Gilman and Foukal (1979) investigated some effects of solar rotation on supergranulation by calculating the convective flow in a thin, rotating spherical shell. They found that fluid parcels tend to conserve their angular momentum as suggested by Foukal and Jokipii (1975) and Foukal (1977) and thus produce mean flows in which the rotation rate of the fluid increases inward. The existence of mean flows such as this is largely confirmed by Duvall's (1980) observations of the rotation rate of the supergranulation cell patterns. It should be noted, however, that fluid parcels need not conserve their angular momentum. Cowling (1951) showed that for nonaxisymmetric convective modes the pressure field can shift in a manner that balances the Coriolis forces and effectively changes the angular momentum of a fluid parcel. The degree to which angular momentum is conserved is highly dependent upon the rotation rate. Explicit calculations, such as those of Gilman and Foukal (1979), are required to determine the direction and magnitude of the angular momentum transport.

The details of the flow within the cells were not examined by Gilman and Foukal (1979) because of limits on the resolution used in their model. In fact they had to use a shell much thicker than that suggested by the horizontal size of the supergranules. In order to study the details of the motions a finer resolution model must be used. In this study a plane parallel model will be used in which a small number of cells are simulated with high resolution. Rotation effects are introduced by including in the momentum equation the Coriolis forces associated with a rotation vector which is tilted from the vertical. The linearized analysis of the onset of convection in such a layer has been examined by Hathaway *et al.* (1979, 1980). The results of these analyses indicate that the tilted rotation vector can produce Reynolds stresses which drive mean flows like those in the nonlinear, spherical shell calculations of Gilman and Foukal (1979). Here a series of nonlinear calculations will be undertaken to examine the details of the flows as well as any global circulations produced by the interaction of rotation with the convective motions. The model will be described in more detail in the second section of this paper followed by a discussion of the results and the observational aspects in the next two sections.

2. The Model

A three-dimensional and time dependent numerical model is used to simulate the convective flow within the supergranules. The geometry employed is shown in Figure 1. A plane parallel layer of fluid is positioned tangent to the sphere at some latitude φ. The effects of curvature are neglected but both the vertical and the horizontal components of the rotation vector are included by tilting the rotation vector from the vertical. A Cartesian coordinate system is used with x increasing toward the east, y increasing toward the north, and z increasing upward, antiparallel to gravity. For simplicity the fluid is assumed to be Boussinesq with the effects of ionization, radiation, and magnetic fields neglected. Although a great deal of

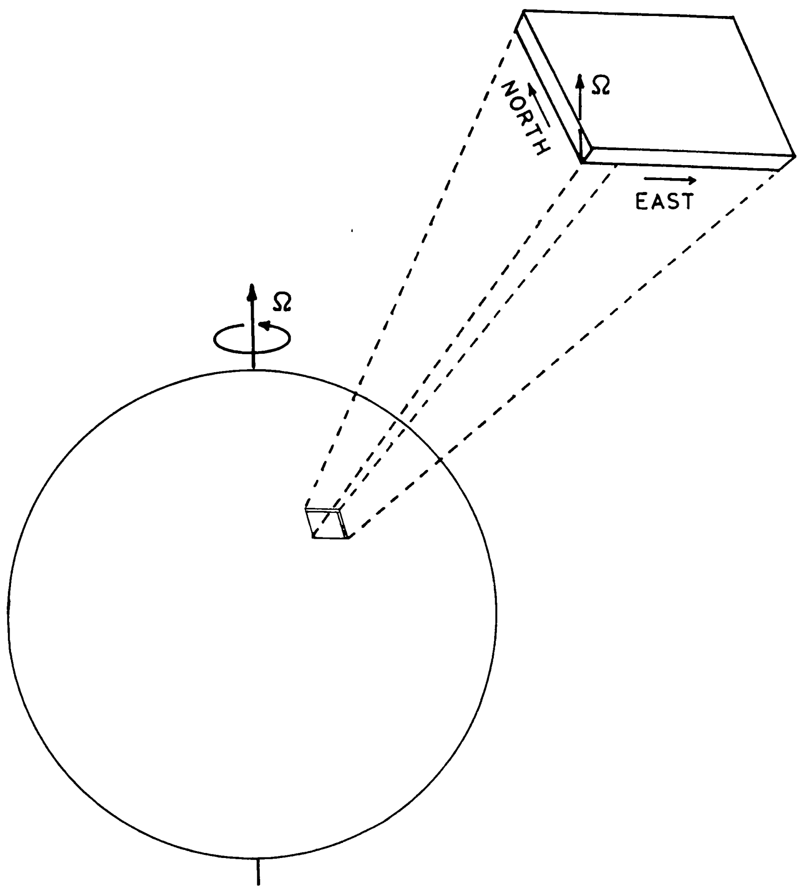

Fig. 1. The plane parallel layer model used in the simulations of the convective flow in supergranulation cells. The rotation vector is tilted from the vertical to represent different latitudes with this model.

interesting physics is lost because of these omissions the resulting simplicity produces a problem which is tractable with present techniques, is more easily analyzed, and provides a framework for future calculations.

A grid point model is used to represent the fluid velocity, temperature, and pressure at discrete points in time. Since the full spectrum of turbulent motions cannot be represented in such a model the subgrid scale motions are parameterized by eddy diffusivities, κ and ν, of heat and momentum, respectively. The full set of equations are then the equation of mass continuity,

$$\frac{\partial u}{\partial x}+\frac{\partial v}{\partial y}+\frac{\partial w}{\partial z}=0\,, \tag{2.1}$$

the three components of the momentum equation,

$$\frac{\partial u}{\partial t}+u\frac{\partial u}{\partial x}+v\frac{\partial u}{\partial y}+w\frac{\partial u}{\partial z}-2\Omega\sin\varphi v+2\Omega\cos\varphi w=-\frac{1}{\rho}\frac{\partial p}{\partial x}+\nu\nabla^2 u\,, \tag{2.2}$$

$$\frac{\partial v}{\partial t}+u\frac{\partial v}{\partial x}+v\frac{\partial v}{\partial y}+w\frac{\partial v}{\partial z}+2\Omega\sin\varphi u=-\frac{1}{\rho}\frac{\partial p}{\partial y}+\nu\nabla^2 v\,, \tag{2.3}$$

$$\frac{\partial w}{\partial t}+u\frac{\partial w}{\partial x}+v\frac{\partial w}{\partial y}+w\frac{\partial w}{\partial z}-2\Omega\cos\varphi u=-\frac{1}{\rho}\frac{\partial p}{\partial z}-(1-\alpha T)g+\nu\nabla^2 w\,, \quad (2.4)$$

and the heat equation,

$$\frac{\partial T}{\partial t}+u\frac{\partial T}{\partial x}+v\frac{\partial T}{\partial y}+w\frac{\partial T}{\partial z}=\kappa\nabla^2 T\,, \quad (2.5)$$

where (u, v, w) is the fluid velocity in the (x, y, z) direction, p is the pressure, T is the temperature, Ω is the rotation frequency and α is the volumetric coefficient of thermal expansion. In applying these equations to astrophysical problems it should be noted that the temperature here is the 'potential temperature' that a fluid element would have if it were adiabatically moved to some reference pressure, i.e., the potential temperature represents temperature differences from an adiabatic distribution.

It is useful to rewrite these equations in a dimensionless form with the basic background distributions of pressure, temperature, and density removed. Taking the depth of the layer, D, as the unit of length, the viscous diffusion time, D^2/ν, as the unit of time, and the temperature difference across the layer, ΔT, as the unit of temperature equations (2.1)–(2.5) become

$$\frac{\partial u}{\partial x}+\frac{\partial v}{\partial y}+\frac{\partial w}{\partial z}=0\,, \quad (2.6)$$

$$\frac{\partial u}{\partial t}+u\frac{\partial u}{\partial x}+v\frac{\partial u}{\partial y}+w\frac{\partial u}{\partial z}-\mathrm{Ta}^{1/2}\sin\varphi v+\mathrm{Ta}^{1/2}\cos\varphi w=-\frac{\partial p}{\partial x}-+\nabla^2 u\,, \quad (2.7)$$

$$\frac{\partial v}{\partial t}+u\frac{\partial v}{\partial x}+v\frac{\partial v}{\partial y}+w\frac{\partial v}{\partial z}+\mathrm{Ta}^{1/2}\sin\varphi u=-\frac{\partial p}{\partial y}+\nabla^2 v\,, \quad (2.8)$$

$$\frac{\partial w}{\partial t}+u\frac{\partial w}{\partial x}+v\frac{\partial w}{\partial y}+w\frac{\partial w}{\partial z}-\mathrm{Ta}^{1/2}\cos\varphi u=-\frac{\partial p}{\partial z}+\frac{\mathrm{Ra}}{\mathrm{Pr}}T+\nabla^2 w\,, \quad (2.9)$$

$$\frac{\partial T}{\partial t}+u\frac{\partial T}{\partial x}+v\frac{\partial T}{\partial y}+w\frac{\partial T}{\partial z}=\frac{1}{\mathrm{Pr}}\nabla^2 T\,, \quad (2.10)$$

where

$$\mathrm{Ta}=\frac{4\Omega^2 D^4}{\nu^2} \quad (2.11)$$

is the Taylor number,

$$\mathrm{Ra}=\frac{\alpha g\Delta T D^3}{\kappa\nu} \quad (2.12)$$

is the Rayleigh number, and

$$\mathrm{Pr}=\frac{\nu}{\kappa} \quad (2.13)$$

is the Prandtl number.

These Equations (2.6)–(2.10) are marched forward in time using an extension of a method first suggested by Chorin (1968) and described in more detail by Somerville and Gal-Chen (1979). The time differencing is implicit to allow larger time steps and the pressure is calculated using an iterative technique. The computer code was originally written for simulating the convective flows realized in laboratory devices and thus employs rigid and conducting top and bottom boundaries. The side boundaries are made periodic as an approximation to an infinite plane parallel layer. The rigid (nonslip) boundaries can maintain stresses which keep the fluid from moving along those surfaces. Although such a mechanism is not expected to be present in the solar atmosphere these boundary conditions have been retained because of the complexity involved in changing to more general boundary conditions. The actual calculations involve 57 600 grid points in an array with 48 points in each horizontal direction and 25 points in the vertical. One time step takes about four seconds on the CRAY-1 computer at NCAR and a typical run takes about 1000 time steps.

Suitable parameter values for these calculations are somewhat uncertain but the observations provide reasonable constraints on their possible ranges. The diffusivities are attributed to the effects of small scale eddies such as granules which, according to mixing length arguments, give values of 10^{12} to 10^{13} cm^2 s^{-1} for both ν and κ. Using constant and equal values for both diffusivities then gives $\mathrm{Pr} = 1.0$. Assuming a layer depth of 20 000 km and using the rotation rate of the Sun of about 27 days gives $\mathrm{Ta} = 5$ to 500. The Rayleigh number is then determined by requiring the maximum horizontal velocities to be about 300 to 500 m s^{-1}. Previous experience with these calculations suggests that $\mathrm{Ra} = 10\,000$ to 50 000 should be sufficient to give velocities of this magnitude while producing a cellular pattern of convection. In order to get a reasonable sampling of cells within the computational domain the horizontal dimensions of the box are taken to be 10 times its depth or about 200 000 km in length.

The actual parameter values may be very different from those used here because of uncertainties in estimating the diffusivities. However, if the ratio of the convective time scale to the rotation period remains about the same the dynamical effects due to rotation will be largely unchanged. Changing the diffusivities will alter the size of the smallest eddies but have little effect on the major characteristics of the largest eddies. This point was made by Hathaway *et al.* (1980) by comparing the dynamics of highly diffusive fluids to those of the inviscid fluids examined in Hathaway *et al.* (1979).

The calculations were started from random temperature perturbations superimposed on a mean temperature field in which the potential temperature decreases linearly with height. An initial run of 1500 time steps was taken with $\mathrm{Pr} = 1.0$, $\mathrm{Ta} = 400$, and $\mathrm{Ra} = 30\,000$ at $\varphi = 90°$. Three parallel calculations of 500 time steps each were then run with the same parameter values at $\varphi = 90°$, 45°, and 15°. The results of these calculations are described in the following section.

Fig. 2. Particle trajectories in three orthogonal planes for the final time step at 90° latitude. The three-dimensional pattern consists of cells with diameters of 30 000 to 50 000 km. The flow on the top surface is from the updrafts (open regions from which the lines diverge) to the downdrafts (dark regions where the lines converge).

3. The Results

The final flow field at $\varphi = 90°$ is shown in a three-dimensional perspective plot in Figure 2. While there is some suggestion of two-dimensional roll-like structures in the particle trajectories plotted here, the dominant form of the motions is that of a cellular pattern with cell diameters of 30 000 to 50 000 km. The maximum velocities attained by the fluid within these cells is about 400 m s^{-1}, giving a typical turnover time of about one day for the convection. These statistics are similar to those given for supergranules by Leighton *et al.* (1962), Simon and Leighton (1964), Worden and Simon (1976), and Giovanelli (1980).

Lifetimes for the cells are obtained by examining the flow patterns at different times. Figure 3 shows the vertical velocity pattern for two points in time separated by about 40 hr. Here solid contours represent upflows and dashed contours represent downflows. Although substantial changes occur in the flow field during the time elapsed there are still enough points of similarity to indicate a somewhat longer lifetime for the cells. A cross correlation analysis of the time series suggests a lifetime of about 200 hr for a typical cell. This is considerably longer than the 40 hr lifetimes found by Worden and Simon (1976) and Duvall (1980) for supergranules.

These lifetimes and velocities indicate that the fluid circulates several times around a cell during its existence in a manner uncharacteristic of supergranules. This fact, together with the hint of two-dimensionality in the flow, indicates that this simulation is not turbulent enough to accurately represent supergranules. However, increasing the Rayleigh number to produce such a state would make the

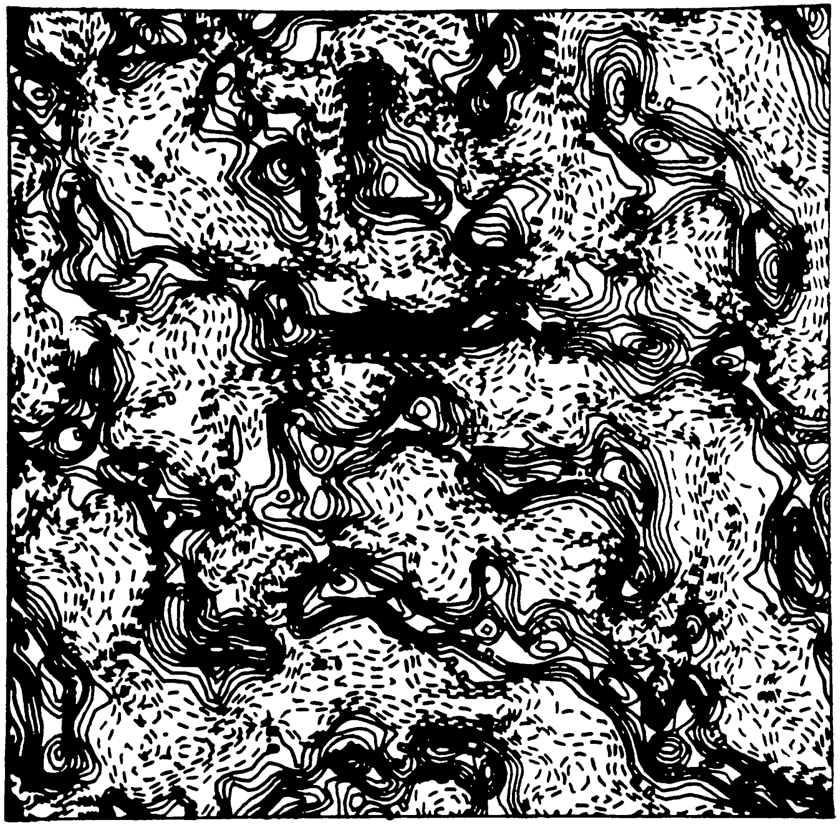

a) t=0 hr

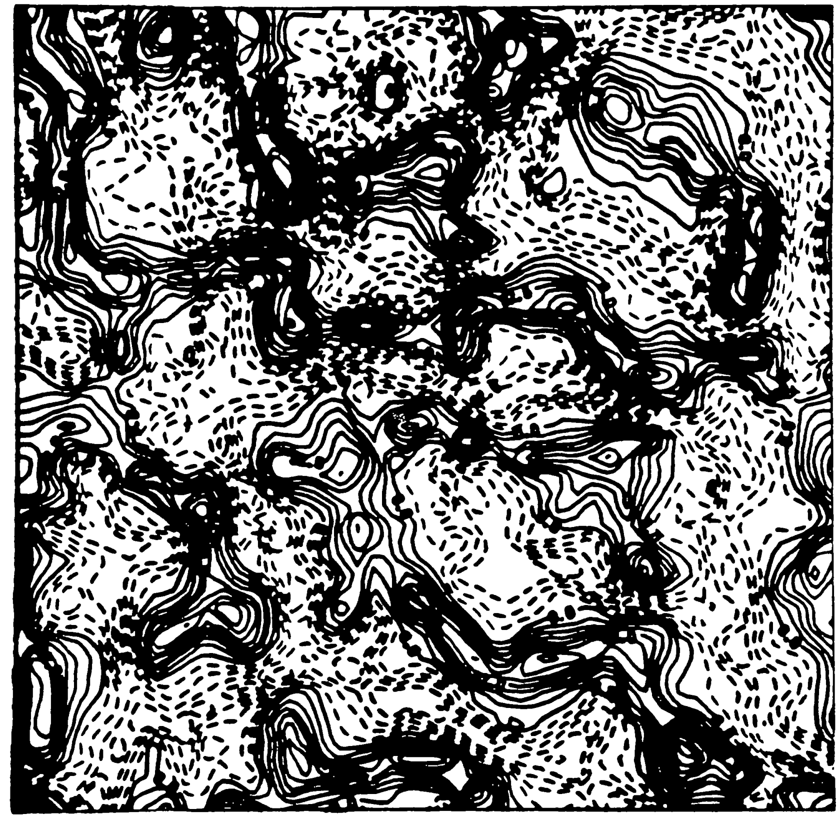

b) t=40 hr

Fig. 3. The time evolution of the vertical velocity field at 90° latitude. Solid contours represent upflows, dashed contours represent downflows. The substantial similarities between these two flow fields separated by 40 hr indicates a somewhat longer lifetime for the cells in this simulation.

velocities and the Coriolis forces too large to realistically describe the effects of rotation on these motions. Several possible changes might make the flow more turbulent while keeping the turnover frequency and the rotation frequency in the same ratio. The simplest would be to decrease the diffusivities by increasing both Ra and Ta. Another possibility would be to change the boundaries to the more realistic stress free conditions. The most important change would be to use a compressible fluid in a layer with several scale heights. This, however, is beyond the scope of the present study.

By requiring the peak velocities to remain between 300 and 500 m s^{-1} while keeping the rotation period at 27 days the turning effect due to the Coriolis forces should be fairly accurately represented in these calculations. Figure 4 shows the particle trajectories in a horizontal plane just below the upper surface for the final flow field at 90° and at 15°. In spite of the long rotation period compared to a turnover time there is substantial turning of the fluid flow. Counter-clockwise (cyclonic) flows are found in the downdrafts (points of convergence in Figure 4) while clockwise (anticyclonic) flows are found in the updrafts. These circulations switch directions in the bottom half of the layer as shown by Veronis (1959), thereby giving a net twisting motion to fluid columns. The magnitude of the vertical vorticity in these flows indicates that a fluid column would gain one complete twist in about one day's time with slightly longer times required in the lower latitudes.

The source of this twisting motion can be determined by examining the vorticity equation. Taking the curl of the momentum Equations (2.7)–(2.9) gives the three components of the vorticity equation

$$\frac{D\xi}{Dt} = +\frac{\text{Ra}}{\text{Pr}}\frac{\partial T}{\partial y} + \xi\frac{\partial u}{\partial x} + (\text{Ta}^{1/2}\cos\varphi + \eta)\frac{\partial u}{\partial y} + (\text{Ta}^{1/2}\sin\varphi + \zeta)\frac{\partial u}{\partial z} + \nabla^2\xi\,, \tag{3.1}$$

$$\frac{D\eta}{Dt} = -\frac{\text{Ra}}{\text{Pr}}\frac{\partial T}{\partial x} + (\text{Ta}^{1/2}\cos\varphi + \eta)\frac{\partial v}{\partial y} + (\text{Ta}^{1/2}\sin\varphi + \zeta)\frac{\partial v}{\partial z} + \xi\frac{\partial v}{\partial x} + \nabla^2\eta\,, \tag{3.2}$$

$$\frac{D\zeta}{Dt} = \underbrace{\phantom{\frac{\text{Ra}}{\text{Pr}}\frac{\partial T}{\partial x}}}_{\text{Buoyancy}} \underbrace{+(\text{Ta}^{1/2}\sin\varphi + \zeta)\frac{\partial w}{\partial z}}_{\text{Stretching}} \underbrace{+(\text{Ta}^{1/2}\cos\varphi + \eta)\frac{\partial \omega}{\partial y} + \xi\frac{\partial w}{\partial x}}_{\text{Tilting}} \underbrace{+\nabla^2\zeta\,,}_{\text{Diffusion}} \tag{3.3}$$

where

$$\frac{D}{Dt} \equiv \frac{\partial}{\partial t} + u\frac{\partial}{\partial x} + v\frac{\partial}{\partial y} + w\frac{\partial}{\partial z} \tag{3.4}$$

and

$$(\xi, \eta, \zeta) = \left(\frac{\partial w}{\partial y} - \frac{\partial v}{\partial z}, \frac{\partial u}{\partial z} - \frac{\partial w}{\partial x}, \frac{\partial v}{\partial x} - \frac{\partial u}{\partial y}\right) \tag{3.5}$$

is the vorticity in the (x, y, z) direction.

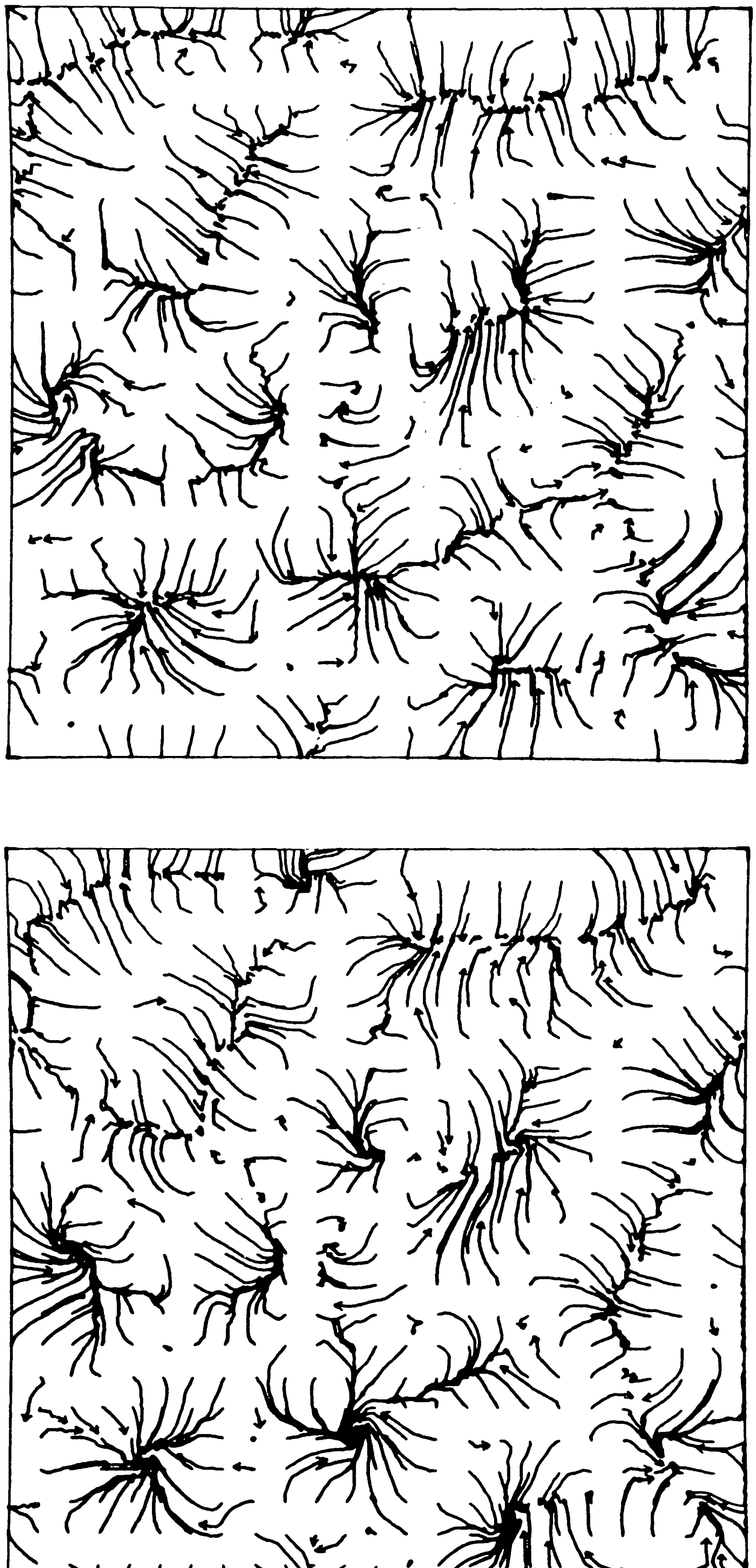

b) $\varphi = 15°$

a) $\varphi = 90°$

Fig. 4. Particle trajectories in a horizontal plane just below the upper surface for (a) 90° latitude and (b) 15° latitude. The twisting motions produced by rotation are much more evident at 90° than at 15° as suggested by a comparison of these two examples.

Horizontal vorticity, ξ and η, is produced primarily by the buoyancy term in Equations (3.1) and (3.2). The turnover frequency of once per day then gives the magnitude of the horizontal vorticity. The vertical vorticity, ζ, is produced by tilting horizontal vorticity into the vertical and then stretching vortex lines. This is an inherently nonlinear process which is not captured in the linear analyses. In the absence of rotation there is no correlation between the sense of vorticity and stretching. However when rotation is included a bias is introduced, as seen in the stretching term in Equation (3.3), which produces a correlation between positive vorticity and stretching. For the case of supergranules this bias is only about 10% of the magnitude of the vertical vorticity but this is sufficient to produce a strong correlation between cyclonic motions and vertical stretching. Thus, from simple physical arguments one would expect twisting frequency for fluid columns to be comparable to a turnover frequency for the slowly rotating case considered here.

The tilted rotation vector used in these calculations can produce anisotropies and systematic Reynolds stresses which drive mean flows. Taking the horizontal average of the flow fields indicates that this indeed occurs. At 90° the mean flows are weak and variable, at 45° they become strong and steady and at 15° they are stronger still. Figure 5 shows the mean flow produced at $\varphi = 15°$. The flow is to the west northwest along the top and to the east southeast along the bottom. The source of these mean flows can be determined from the horizontally averaged momentum equations. Taking the horizontal average of Equations (2.7) and (2.8) gives

$$\frac{\partial \bar{u}}{\partial t} = -\frac{\partial}{\partial z}\overline{uw} + \mathrm{Ta}^{1/2} \sin \varphi \bar{v} + \frac{\partial^2 \bar{u}}{\partial z^2} \tag{3.6}$$

and

$$\frac{\partial \bar{v}}{\partial t} = -\frac{\partial}{\partial z}\overline{vw} - \mathrm{Ta}^{1/2} \sin \varphi \bar{u} + \frac{\partial^2 \bar{v}}{\partial z^2}, \tag{3.7}$$

where the overbar indicates horizontally averaged quantities. For a steady-state solution the terms on the right-hand sides of Equations (3.6) and (3.7) must be in balance. Figure 5 shows that in the upper half of the layer and the last two terms in Equation (3.6) are positive so these must be balanced by a negative contribution from the first term on the right hand side. At the equator the middle term vanishes so the primary balance must be between the Reynolds stress $\overline{uw}$ and the vertical gradient of the zonal velocity $\partial\bar{u}/\partial z$. This Reynolds stress is readily attributed to the action of the Coriolis force on the convective motions. The horizontal component of the rotation vector produces a Coriolis force on the vertical flow such that upward moving elements conserve their angular momentum and are forced to the west. The resulting correlation between upward flows and westward motions then drives a mean flow in which the rotation rate increases inward.

A similar analysis of Equation (3.7) shows that in the upper half of the layer the last term is negative while the middle term is positive. Inspection of the magnitudes

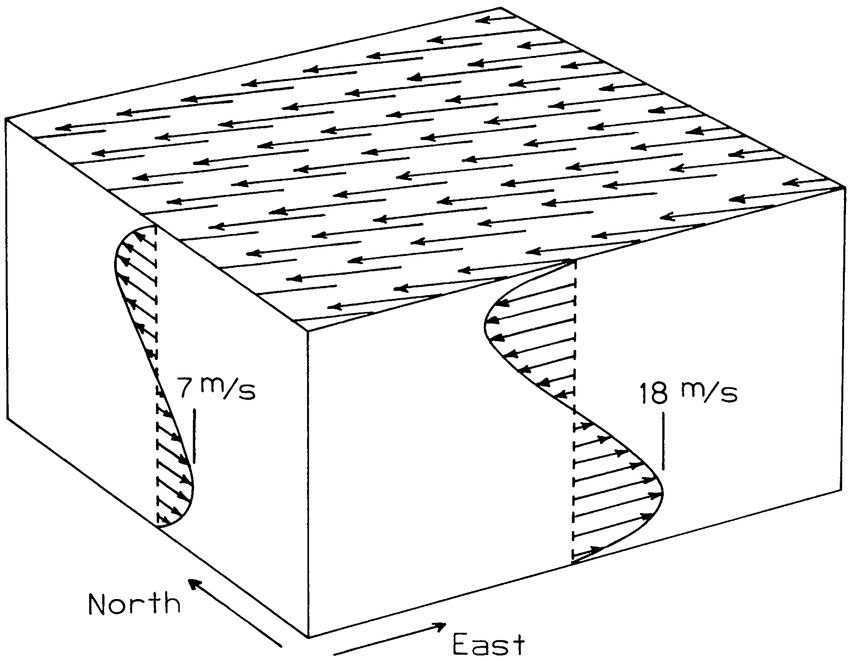

Fig. 5. The mean flow produced at 15° latitude. The east-west flow produced here gives a rotation rate which increases inward. The resultant meridional circulation has a poleward flow along the upper surface.

of these two terms shows that a partial balance can exist between the production of the meridional flow by the Coriolis force acting on the mean zonal flow and the destruction of the meridional flow by diffusion. However even here the Reynolds stress term, $\overline{vw}$, is important for producing the mean circulation. The Coriolis forces due to the horizontal component of the rotation vector produces a correlation between upward and westward motions. Similarly the Coriolis forces due to the vertical component of the rotation vector produces a correlation between westward and poleward motions. The net effect is a correlation between upward and poleward flows which contributes to the production of the meridional circulation.

This analysis indicates that the production of mean flows, such as that shown in Figure 5, can be attributed primarily to the conservation of angular momentum by upward moving elements. Such a conclusion was also reached by Gilman and Foukal (1979) and should be independent of boundary conditions or the mean density distribution.

4. Observational Aspects

The twisting motions produced by the effects of rotation should be observable in the velocity fields within the supergranules. Figure 6 shows particle trajectories for a simple hexagonal pattern both with and without Coriolis forces. As noted earlier the stretching of vortex lines produce clockwise motions around downdrafts and counter-clockwise motions around updrafts in the northern hemisphere. If these

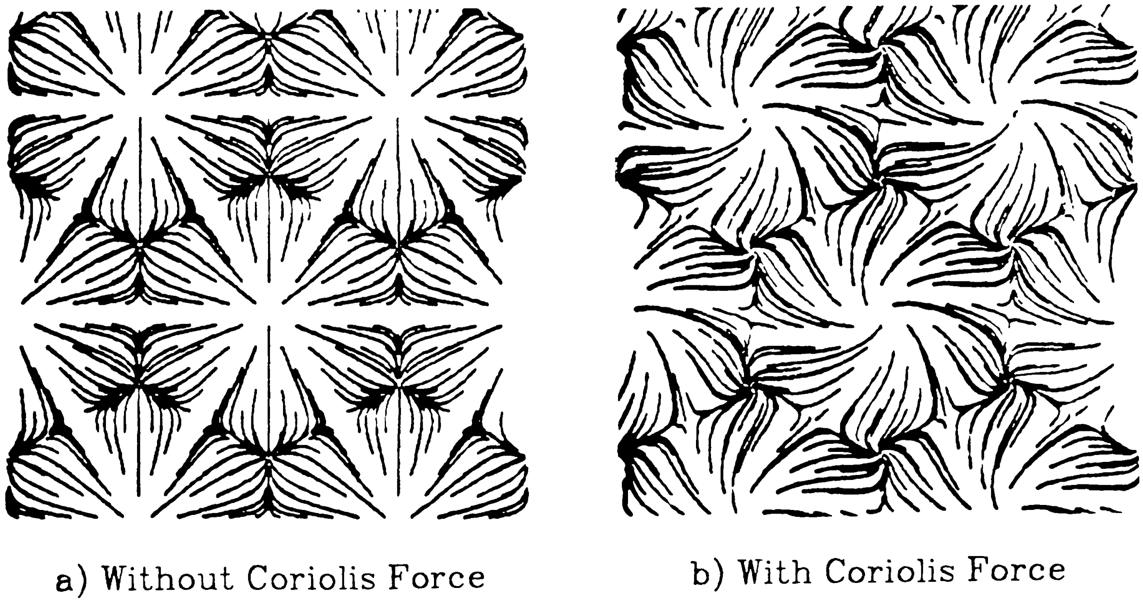

Fig. 6. Particle trajectories for regular hexagonal cells (a) in the absence of rotation and (b) in the presence of rotation. Clockwise (anticyclonic) flows are produced in the updrafts while counter-clockwise (cyclonic) flows are produced in the downdrafts.

velocity fields are viewed from an oblique angle the line of sight velocities will produce patterns like those in Figure 7. Here the unshaded regions represent flows toward the observer while the shaded regions represent flows away from the observer. In the absence of rotation the zero velocity line through the cell centers separating regions of approaching and receding velocities, is parallel to the limb.

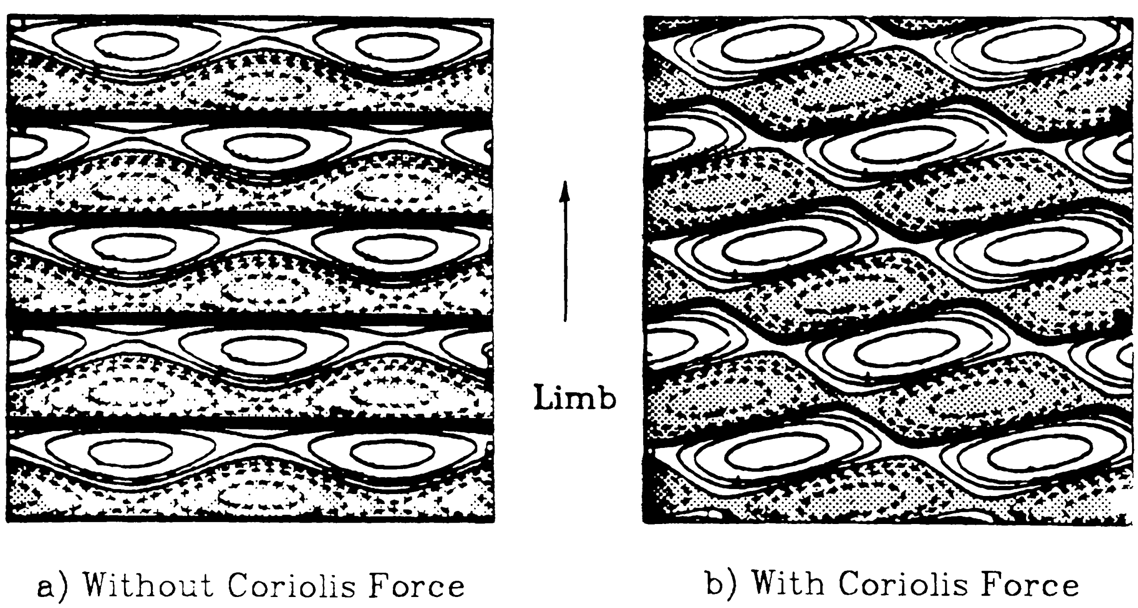

Fig. 7. The line of sight velocities produced by the flow fields represented in Figure 6. Without rotation the line of zero velocity between approaching fluid (unshaded regions) and receding fluid (shaded regions), is parallel to the limb as shown by the heavy line through the cell centers in (a). With rotation this line gets tilted in one direction in the upflows and the other direction in the downflows as in (b).

In the presence of rotation this line gets tilted, with one sense of tilting in updrafts and the other in downdrafts, to reflect the different sense of the circulations around these regions.

Kubicela (1973) reports seeing such a tilt near the center of the cells but makes no mention of tilting of the other sense near the downdrafts. This lack of observational evidence for the cyclonic flows around the downdrafts may be due to the fact that it is somewhat unexpected from simple arguments concerning the Coriolis forces. (These cyclonic flows are produced by the stretching of vortex lines in regions of convergent flows.) However it may also be that the downdrafts are concentrated into smaller areas and thus harder to observe. For the Boussinesq fluid used in this model the updrafts and downdrafts cover similar areas as seen in Figure 2. Although the observations are somewhat confused by the presence of magnetic structures it does appear that on the Sun the downdrafts are stronger and more concentrated than the updrafts. If this is indeed the case then it must be produced by the additional effects of compressibility or magnetic fields.

The difficulty in observing these motions is indicated in Figure 8 where the line of sight velocities from the flow field at 45° are shown in the same manner used in Figure 7. Since the tilt of the zero velocity line is different for updrafts and downdrafts the resulting pattern is very complicated. Such patterns will certainly require a clever form of analysis to extract the subtle effects of rotation.

The existence of mean flows like that shown in Figure 5 is perhaps better established. Foukal and Jokipii (1975), Foukal (1977), and others have suggested

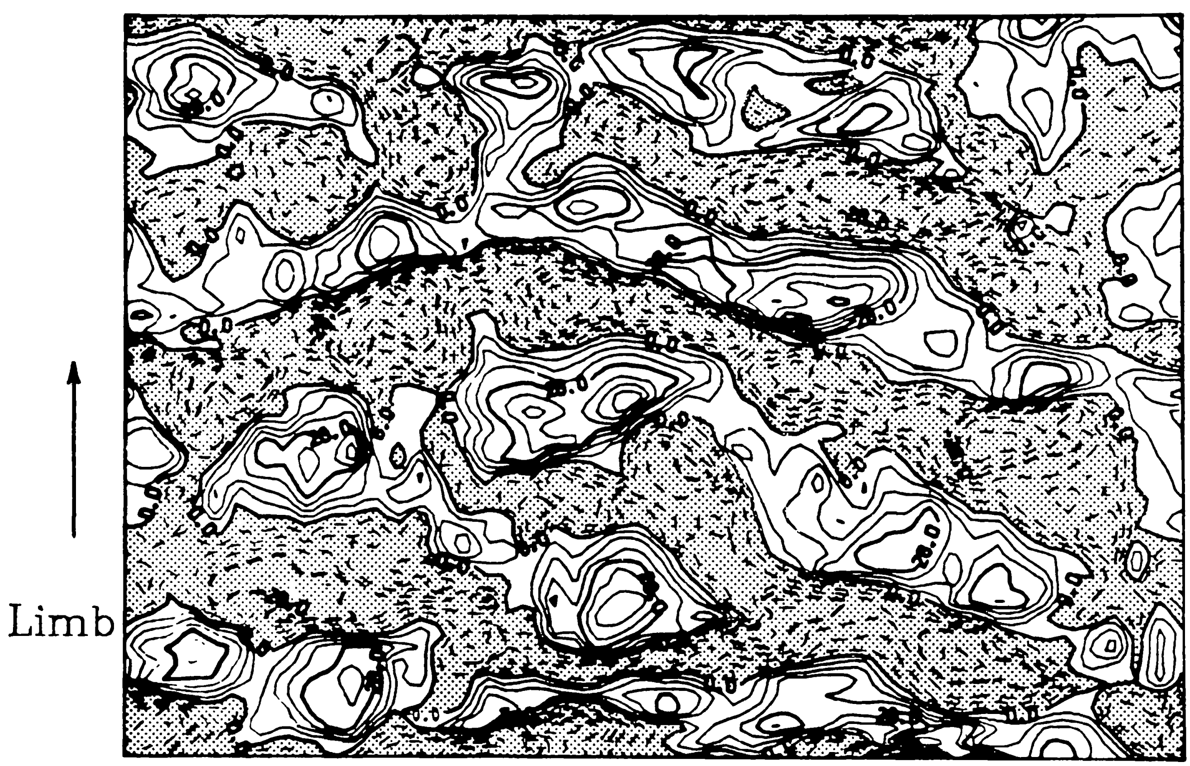

Fig. 8. The line of sight velocities at 45° latitude from the flow fields produced in the simulations. The tilting of the line of zero velocity is difficult to see in these more complex patterns.

that the observed rotation rate of magnetic fields indicates a rotation rate that increases with depth. Duvall (1980) has found that the supergranular velocity pattern itself also rotates at a faster rate than the photosphere. The suggestion that this may be due to fluid elements conserving their angular momentum as they move upward is born out by the results of this study and that of Gilman and Foukal (1979).

The existence of a meridional circulation like that found here is less well established. The circulation is of small amplitude, typically about $10 \mathrm{~m~s}^{-1}$, and thus difficult to observe. Howard (1979) and Duvall (1979) both report observations of a meridional circulation of the same sense and of similar magnitude to that produced here. However Beckers and Taylor (1980) suggest that corrections due to the limb effect may substantially change the observed magnitude. Certainly better observations of the flows within the supergranules and the mean flows they produce will be useful for providing further constraints on dynamical models of this phenomena.

5. Conclusions

The interaction of solar rotation with the convective flow in supergranulation cells has important dynamical consequences for the Sun. This is somewhat unexpected in view of the Sun's slow rotation rate compared to an overturning time for the convection. Nonlinear effects tilt the vorticity in the overturning motions into the vertical and then magnify them by stretching to produce twisting motions in the updrafts and downdrafts. For the incompressible fluid used in this model the twisting is large enough to produce one complete turn in one day. Compressible fluids can produce much stronger twisting motions. Glatzmaier and Gilman (1981) show that a major source of vorticity in a rotating compressible fluid is due to the compression and expansion of a fluid element as it moves radially. This effect produces an additional source of convergence and divergence for magnifying the vertical vorticity. Such motions will certainly have important effects on the magnetic fields in the fluid. The concentration and twisting of magnetic fields in the cell boundaries may very well produce magnetic structures similar to spicules. Hollweg (1980) has suggested that the subsequent release of energy associated with these twists may contribute to coronal heating.

The horizontal component of the rotation axis introduces systematic Reynolds stresses which drive mean flows. As the fluid moves upward it conserves its angular momentum and is forced to the west. This correlation between upward and westward flows drives a mean flow which is directed to the west on top and to the east along the bottom of the layer. Such a flow represents a differential rotation in which the rotation rate increases inward in agreement with Duvall's (1980) observation of the motion of the supergranulation cell patterns. The Coriolis force acting on this mean flow together with the correlation between westward and poleward flows then drives a somewhat weaker meridional circulation with poleward flow near the upper surface and equatorward flow along the bottom.

The magnitudes of the velocities predicted from these calculations cannot be taken at face value because of the approximations made. Gilman (1978) has shown that by using stress free boundaries, instead of the rigid ones used here, the magnitude of the resulting velocities can be substantially changed. More importantly, the use of a compressible fluid with large density variations between the top and the bottom will certainly alter the velocity amplitudes. However, one would not expect these changes to alter the sense of the mean flows or the physical mechanisms by which they are produced.

These mean flows should be coupled with those produced by giant cell convection. Gilman (1977) finds that the strong rotational constraint on very large scale convection produces a differential rotation in which the rotation rate decreases with depth. Since this is in the opposite sense to the circulation produced here the superposition of the two should give a maximum in the rotation rate somewhere near the bottom of the supergranulation layer. The meridional circulation produced in Gilman's (1977) calculations is in the same sense as that found in this study. Thus, the net effect should be an enhancement of the poleward flow near the surface with a strong decrease or even a counter flow near the bottom of the supergranulation layer.

These results indicate that careful consideration of solar rotation effects on the small scale motions should be included in global dynamical models for the Sun. The flows produced at the surface can be altered by these effects and should be included in some form if models are to be seriously compared to observations. Realistic models of the full effects should include compressibility and magnetic fields but the qualitative features suggested by the results of these calculations should be relatively independent of any effects produced by these additions.

Acknowledgements

I am deeply indebted to Richard Somerville and Tzvi Gal-Chen who supplied the original version of the computer code used in this study. I would also like to express my sincere appreciation to Juri Toomre and Peter Gilman for a number of useful discussions on the scientific aspects. I should also thank Gordon Newkirk whose questions about the amount of twisting produced by solar rotation provided the initial impetus for this work.

These calculations were carried out while I was a fellow in the Advanced Study Program and a visitor in the High Altitude Observatory of the National Center for Atmospheric Research. Some of the work on the observational aspects was undertaken while I was a summer student at Sacramento Peak Observatory. I am very grateful for the support provided by these institutions and their sponsor, the National Science Foundation.

References

Beckers, J. M. and Taylor, W. R.: 1980, *Solar Phys.* **68**, 41.
Chorin, A. J.: 1968, *Math. Comput.* **22**, 745.
Cowling, T. G.: 1951, *Astrophys. J.* **114**, 272.
Duvall, T. L.: 1979, *Solar Phys.* **63**, 3.

Duvall, T. L.: 1980, *Solar Phys.* **66**, 213.
Foukal, P. V.: 1977, *Astrophys. J.* **218**, 539.
Foukal, P. V. and Jokipii, J. R.: 1975, *Astrophys. J. Letters* **199**, L71.
Gilman, P. A.: 1977, *Geophys. Astrophys. Fluid Dynam.* **8**, 93.
Gilman, P. A.: 1978, *Geophys. Astrophys. Fluid Dynam.* **11**, 181.
Gilman, P. A. and Foukal, P. A.: 1979, *Astrophys. J.* **229**, 1179.
Giovanelli, R. G.: 1980, *Solar Phys.* **67**, 211.
Glatzmaier, G. A. and Gilman, P. A.: 1981, *Astrophys. J. Suppl.* **45**, in press.
Hart, A. B.: 1954, *Monthly Notices Roy. Astron. Soc.* **114**, 17.
Hart, A. B.: 1956, *Monthly Notices Roy. Astron. Soc.* **116**, 38.
Hathaway, D. H., Gilman, P. A., and Toomre, J.: 1979, *Geophys. Astrophys. Fluid Dynam.* **13**, 289.
Hathaway, D. H., Toomre, J., and Gilman, P. A.: 1980, *Geophys. Astrophys. Fluid Dynam.* **15**, 7.
Hollweg, J. V.: 1980, *Bull. Am. Astron. Soc.* **12**, 909.
Howard, R.: 1979, *Astrophys. J. Letters* **228**, L45.
Kubicela, A.: 1973, in J. Xanthakis (ed.), *Solar Activity and Related Interplanetary and Terrestrial Phenomena*, Proceedings of the First European Astronomical Meeting, Springer-Verlag, p. 123.
Leighton, R. B., Noyes, R. W., and Simon, G. W.: 1962, *Astrophys. J.* **135**, 474.
Simon, G. W. and Leighton, R. B.: 1964, *Astrophys. J.* **140**, 1120.
Somerville, R. C. J. and Gal-Chen, T.: 1979, *J. Atmospheric Sci.* **36**, 805.
Veronis, G.: 1959, *J. Fluid Mech.* **5**, 401.
Worden, S. P. and Simon, G. W.: 1976, *Solar Phys.* **46**, 73.